



Showcasing research from Professor Jungil Choi's laboratory, Department of Mechanical Engineering, Ajou University, Suwon, Republic of Korea.

Rapid antimicrobial susceptibility testing for low bacterial concentrations integrating a centrifuge based bacterial cell concentrator

A rapid antibiotic susceptibility test (AST) platform that allows the use of low-density bacterial samples by concentrating bacterial cells and performing AST on a single microfluidic chip was developed.

As featured in:



See Sunjae Hwang and Jungil Choi, *Lab Chip*, 2023, **23**, 229.


 Cite this: *Lab Chip*, 2023, 23, 229

Rapid antimicrobial susceptibility testing for low bacterial concentrations integrating a centrifuge based bacterial cell concentrator†

 Sunjae Hwang^a and Jungil Choi ^{*b}

Antibiotic resistance threatens human health worldwide. Patients infected with antibiotic-resistant bacteria require appropriate antibiotic prescriptions based on a rapid antibiotic susceptibility test (AST). Various rapid AST methods have been developed to replace the conventional AST method, which requires a long testing time. However, in most cases, these methods require a high density of bacterial samples, which leads to an additional incubation or concentration process. In this study, we introduce a rapid AST platform that allows the use of low-density bacterial samples by concentrating bacterial cells and performing AST on a single microfluidic chip. In addition, the outlet-free loading process enables the platform to load the sample and concentrate bacteria into a small field of view for single-cell detection. Using this method, rapid AST determined antibiotic resistance in three hours from a standard strain of 10^3 colony-forming unit (CFU) per ml bacterial concentration. This technique can be used for the cell-based drug testing of various low-concentration bacterial samples.

 Received 18th October 2022,
 Accepted 1st December 2022

DOI: 10.1039/d2lc00974a

rsc.li/loc

1. Introduction

Antibiotic resistance is increasing rapidly worldwide.¹ Because the management of COVID-19 increasingly relies on pharmacological interventions, a huge risk of increasing antimicrobial resistance has been reported.² Due to the increase in antibiotic-resistant bacterial strains in clinical practice, antimicrobial susceptibility testing (AST) is required to determine the antibiotic resistance exhibited by a patient and a prescription suitable for the patient.³ The AST methods are divided into genotype and phenotype methods. In the case of the genotype method, rapid diagnosis is possible because it uses genetic information of the bacteria without an additional bacterial culture process.⁴ However, there are cases where the results of the genotype method differ depending on whether it is actually resistant or not.⁵ Phenotypic resistance has distinct enzymes that can vary depending on the level of expression as well as the presence of genes. Therefore, in actual clinical practice, a phenotypic method for observing bacterial reactions through culture is adopted as the standard method.⁶

The standard AST method is the broth microdilution (BMD) test; commercial methods used in the field are MicroScan (Beckman Coulter, Sacramento, CA) and Vitek 2 (bioMérieux, Durham, NC). In both cases, antibiotic sensitivity is determined by the degree of bacterial division while culturing bacteria in an antibiotic solution, which requires overnight incubation.⁷ The long culturing time of AST hinders the appropriate treatment of sepsis patients who need rapid prescription of antimicrobial drugs.⁸

To address this issue, rapid AST methods have been developed through many studies by integrating microfabrication, image processing, electrochemistry, and nanotechnology.^{9,10} The many of the phenotype rapid AST methods directly determine the response of bacteria to antimicrobials through microscopic observation of the growth of bacteria.^{11–17} In addition, various methods of phenotypic AST have been reported,¹⁸ including electrical measurements,¹⁹ label-free scattering technologies (light scattering²⁰ and Raman²¹), detecting the vibrations of a cantilever by bacteria,²² electrochemical sensing,^{23,24} atomic force microscopy,²⁵ and fluorescence-activated cell sorting (FACS).²⁶ These approaches dramatically reduce the time of AST from a few hours to 30 min.

However, because these rapid AST methods are based on microscopic observation of bacteria or micro/nano scale sensors, a high concentration of bacteria in samples, approximately 10^7 – 10^8 colony-forming units (CFU) per ml, is required for testing. Usually, a few bacterial colonies from an agar plate are diluted to the target concentration to prepare the

^a Department of Mechanical Engineering, Kookmin University, Seoul 02707, Republic of Korea

^b Department of Mechanical Engineering, Ajou University, Suwon 16499, Republic of Korea. E-mail: cji@ajou.ac.kr

† Electronic supplementary information (ESI) available. See DOI: <https://doi.org/10.1039/d2lc00974a>

sample for rapid AST. The reason for the requirement of high-density bacterial samples is the poor detection limit of these methods. For example, in the case of microscopy imaging analysis, magnification of at least $40\times$ is required for accurate bacterial observation. In this case, since the field of view of the image is $150 \times 150 \mu\text{m}$, 10^8CFU ml^{-1} or higher is required to obtain images of dozens of bacteria for the stable observation of bacterial growth. The first method is to increase the concentration of bacteria through an additional culture process. This method is used to obtain bacteria by culturing blood samples from patients with bacteremia. In the urine sample, if the concentration is 10^5CFU ml^{-1} or higher, it is determined to be positive infection, and in this case it is difficult to apply rapid AST immediately since additional culture is required. This additional culture does not help the overall purpose of rapid AST, because it requires more time.

Another method involves concentrating the sample using a centrifuge and then using the concentrated sample for rapid AST. Even though this method is widely used,²⁷ this process requires an additional sample processing step, so there is a chance of sample loss during pretreatment and inconvenience to the user. It takes time and effort because after the enrichment process, the sample must be placed into the AST platform. Therefore, for rapid AST of low-concentration bacterial samples, a new method is needed that can process the low-concentration bacteria in one platform. In the field of lab on a chip, there are many applications using centrifuge microfluidic devices.²⁸ In most cases, centrifugal force was used for loading liquid samples into separate testing chambers.²⁹ A microfluidic disc system used binding of pathogens to antibody-functionalized particles for the sedimentation of the particles through density media.³⁰ A disc-based platelet isolation system used two filter sizes to separate platelets from red blood cells and bacteria.³¹ A fidget spinner-based point of care testing system used a filter for the concentration of bacteria in a sample

from a patient with urinary tract infection.³² The system was used for AST but it required an antibiotic exposure process on the outside of the chip.

In this study, we introduce a platform for performing rapid AST by injecting low-concentration bacterial samples into a microfluidic chip and then concentrating the bacteria into small areas of observation through centrifugal force (Fig. 1). Low-concentration bacterial samples were loaded onto microfluidic chips, and bacterial concentration, culture, and AST processes were performed as a one-step process on a single chip. The response of bacteria to antimicrobials was analyzed using microscopy imaging to determine antibiotic susceptibility. In addition, to provide the user convenience and prevent sample loss, an outlet-free sample loading method was developed to ensure convenience in sample loading. Through experiments on standard strains, it was demonstrated that rapid and accurate AST can be performed in three hours at a bacterial sample concentration of 10^3CFU ml^{-1} .

2. Materials and methods

Design and fabrication of the microfluidic chip

The microfluidic channel chip was designed using a 3D CAD program (SolidWorks, Dassault Systems, France). The chip was made of two materials: a plastic chip with a diameter of 100 mm and a polyethylene terephthalate (PET) cover film with a thickness of $150 \mu\text{m}$. The distance from the center to the end of the channel is 45 mm and the depth of the channel is $450 \mu\text{m}$. The chip was designed for a single use and could be mass-produced. Injection molding formed the chips with plastic material general-purpose polystyrene (25SP, LG Chem., Seoul, Republic of Korea). The annular shaped chip was sealed using an adhesive PET cover film, obtained from a punching process (Fig. 2). At the end of each microfluidic channel, there is a bacterial trap with a size of $150 \times 250 \mu\text{m}$ with a depth of $50 \mu\text{m}$.

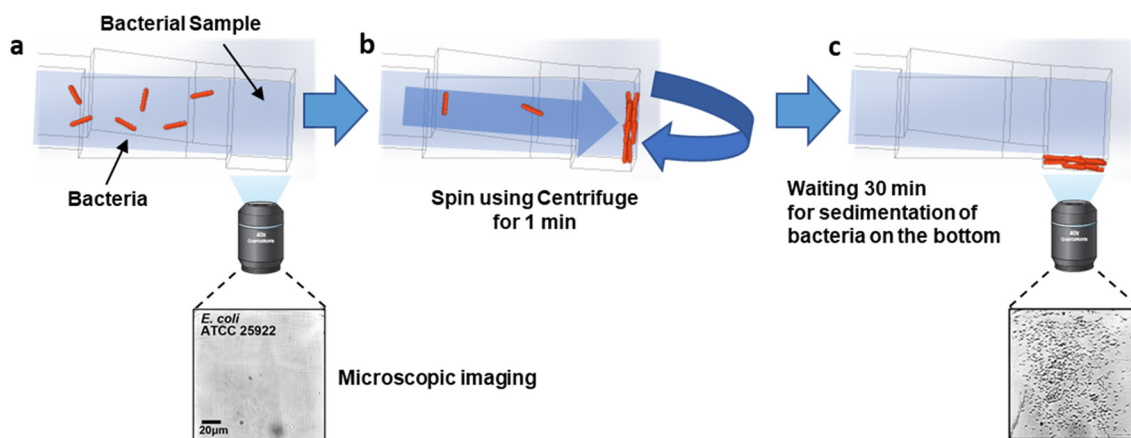


Fig. 1 Schematic of the concentration process using centrifugal force in the microfluidic chip. (a) Bacterial sample at low concentration was loaded in the channel of the chip. Bacteria could not be identified in the microscopy image due to the low concentration of bacteria in the sample. (b) The chip was subjected to a concentration process by rotating it using a centrifuge for 1 min. In this process, bacteria that had spread throughout the long channel were collected on the wall at the end of the channel. (c) After 30 min of centrifuge, the bacteria settled to the bottom of the channel. After imaging through a microscope, it was confirmed that the bacteria were significantly concentrated.

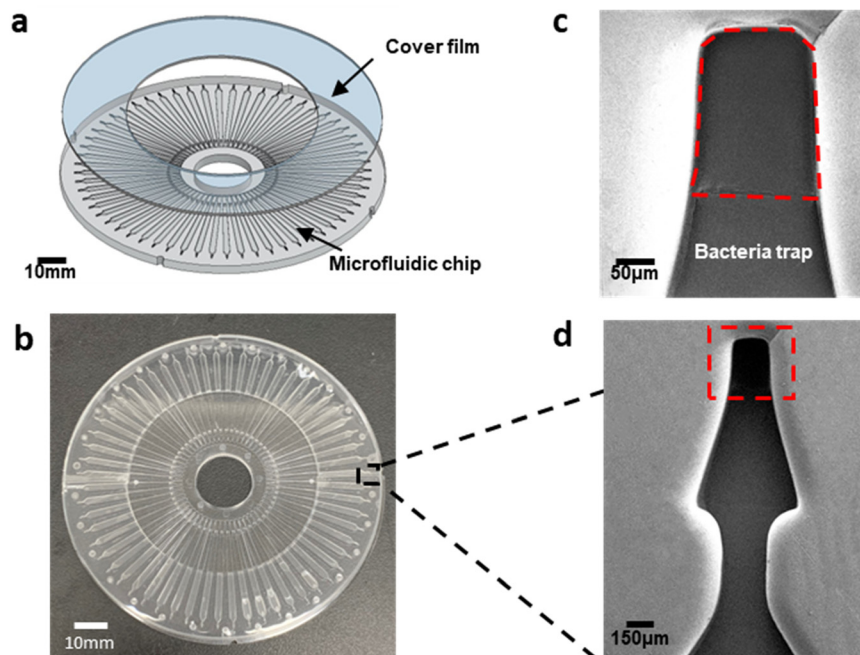


Fig. 2 Device for the centrifugal antimicrobial susceptibility testing (AST). (a) Schematic of the chip. (b) Image of the chip. (c and d) SEM images of the microfluidic channel and bacteria trap.

Preparation and AST process of the microfluidic AST chip

An antibiotic solution (5 μl of antibiotic solution in distilled water) was loaded into the small well of the microfluidic channel of the chip (Fig. 3a and S1a \dagger). The chip was placed in a natural flow type oven (ThermoStable™ ON-105; Daihan Scientific, Seoul, Republic of Korea) at 50 °C for 15 min to dehydrate the antibiotics in the channel (Fig. 3b and S1b \dagger). A circular PET film covered the region of dried antibiotics to protect the antibiotics from plasma treatment (Fig. 3c and S1c \dagger). The microfluidic channel chip containing antibiotics was treated with oxygen plasma (CUTE-MP, Femto-Science, Republic of Korea) at 100 W for 30 s to create a hydrophilic microfluidic chip (Fig. 3d and S1d \dagger). A thermal laminating machine (Sindoh Techno, TL-6600, Seoul, Republic of Korea) bonded the PET film onto the microfluidic channel chip at 70 °C and at a low speed (Fig. 3e and S1e \dagger).

After the preparation of the microfluidic AST chip, a bacterial sample (10 μl) was injected into the channel through the chip inlet (Fig. 3f and S2a \dagger). The technique, we named it the outlet-free-loading technique, was used to inject bacterial samples without an outlet. A vacuum pump (Roker 300, Taiwan) at 300 mbar and a vacuum chamber were used to remove the air in the channel of the chip (Fig. 3g and S2b \dagger). After degassing, the chip was placed at atmospheric pressure and the bacterial sample was then transferred into the microfluidic channel (Fig. 3h). An aluminum chuck with four pins at the corners made by a CNC machining process held the microfluidic concentration chip on the centrifuge (Fig. S3a \dagger). The chuck was assembled to a centrifuge (Daihan Scientific, CF-10, Republic of Korea) (Fig. S3b and c \dagger). The

chip was rotated for 1 min at 11 000 rpm (6098 RCF) using a centrifuge (Fig. 3i and S2c \dagger). After rotation, the bacteria were concentrated on the wall and slowly sank to the bacterial trap. The bacteria were observed using an inverted optical microscope (IX70, Olympus, Japan) with a 40 \times optical lens (LCPlanFI, Olympus, Japan) (Fig. 3j and S2d \dagger). Time-lapse images of bacterial growth were taken every 30 min.

Bacterial strains

Three standard Clinical and Laboratory Standards Institute (CLSI) bacterial strains, *Escherichia coli* (ATCC 25922), *Staphylococcus aureus* (ATCC 29213), and *Enterococcus faecalis* (ATCC 29212), were obtained from Kwik-Stik (Cat. no. 0335P, 0365P, 0366P, Microbiologics, Minnesota, USA). Bacterial stock solutions were prepared using 25% glycerol (Sigma Aldrich, Massachusetts, USA) and stored in a deep freezer (UniFreez, Fre80-86, Daihan Scientific, Republic of Korea) at -70 °C. The bacterial strains were cultured on LB agar plates (Kisan Bio, Seoul, Republic of Korea) for 20 h in an incubator at 37 °C before the test. Bacterial samples were prepared at concentrations of 0.5 McFarland (McF) (5×10^8 CFU ml^{-1}) using a nephelometer (Densichek Plus Standards, BIOMÉRIEUX). Subsequently, this bacterial sample was serially diluted with a Mueller Hinton Broth (MHB) culture medium (BBL™, BD, USA) to the target concentrations of the test (10^3 and 10^4 CFU ml^{-1}).

Antibiotics preparations

All antibiotics were purchased from Merck (Sigma-Aldrich, Massachusetts, USA). Stock solutions were prepared using

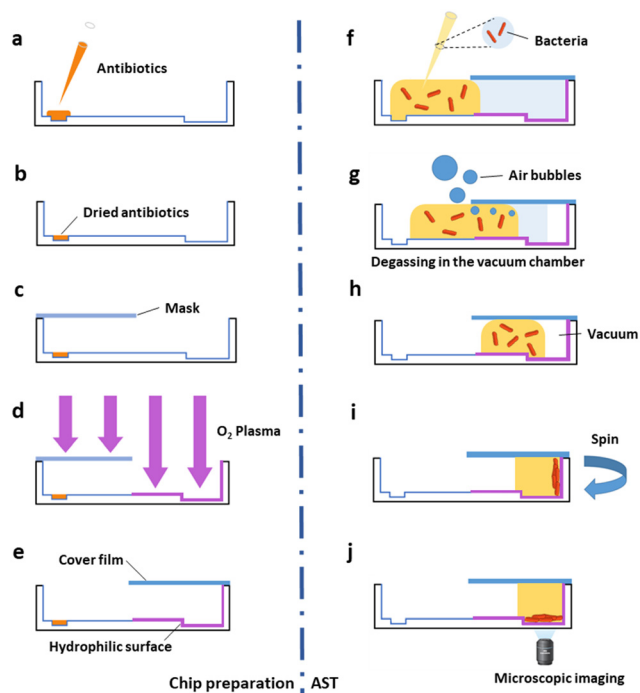


Fig. 3 Process of preparing the AST chip (a–e) and performing AST (f–j). (a) Antibiotics are loaded into the reservoir in the chip. (b) Antibiotics are dehydrated by heat in the oven. (c) The chip is covered with a mask to protect the antibiotics. (d) Oxygen plasma treatment to make channels partially hydrophilic. (e) The chip is sealed with a film to make the centrifuge chip. (f) Bacterial samples are injected into the channel. (g) Discharging the air inside the channel. (h) After degassing, the chip is placed at atmospheric pressure. The bacterial sample moves to the vacuum channel covered with the film. (i) The chip is rotated by using a centrifuge to concentrate the bacteria. (j) After the bacteria have completely sunk on the bacterial trap, bacterial growth is tracked by using a microscope in a time lapse imaging method.

DIW and stored at $-70\text{ }^{\circ}\text{C}$. The solutions were thawed to room temperature and diluted to the target concentration in DIW.

Broth microdilution test

The BMD test was conducted according to the criteria provided by the CLSI and was used as the gold standard. Stock solutions of antibiotics were prepared and diluted to the appropriate concentration, which was determined using the CLSI criteria. One hundred microliters of the antibiotics were pipetted into the wells of 96 MicroWell plates (Falcon, BD Biosciences). Ten microliters of bacterial solution ($5 \times 10^5\text{ CFU ml}^{-1}$) were inoculated into the wells. After preparation, the well plates were incubated at $37\text{ }^{\circ}\text{C}$ for 20 h. The MIC values were determined by comparing the turbidity of the wells with antibiotics with that of the wells without antibiotics. When the number of bacteria grew up to 20% larger than the number of bacteria in the control volume, that concentration was adopted as the growth value following the guideline from the CLSI for broth microdilution test.⁶

Colony counting

The optical density of the bacterial sample was measured to determine the number of bacteria present in the MHB culture medium. However, even at the same optical density, the actual number of bacteria differed depending on the bacterial type. For example, in the case of *S. aureus*, there were approximately 2.6 times more colony forming units than *E. faecalis* at the same McFarland (McF) nephelometer value. To solve this problem, colony counting was performed. It was assumed that there were $1.5 \times 10^8\text{ CFU}$ in 1 ml of the bacterial sample when the value measured by the nephelometer was 0.5 McF. The samples were diluted and adjusted to a bacterial concentration of $1 \times 10^3\text{ CFU ml}^{-1}$. Next, $100\text{ }\mu\text{l}$ of the diluted sample was loaded onto an agar plate and spread evenly. After the sample was absorbed by agarose, it was incubated overnight. After incubation, the bacteria present in the sample formed colonies and their numbers were counted. To determine the accuracy of this test, three tests were performed on each sample (Fig. S4 and Table S1†).

Centrifugal concentration process

The concentration of the bacterial sample loaded on the chip was set to the minimum concentration at which the bacteria could be identified in the image after concentration. The test was conducted at a sample concentration range of 10^1 – 10^5 CFU ml^{-1} . When $10\text{ }\mu\text{l}$ of the 10^4 CFU ml^{-1} bacterial sample was loaded and concentrated, 100 bacterial cells were observed under a microscope. To verify the effect of the bacterial concentration, the numbers of bacteria in the loaded sample and in the microscopy image after concentration were compared. The bacterial concentration of the bacterial sample was 10^4 CFU ml^{-1} , and the final number of bacteria was 100 by loading $10\text{ }\mu\text{l}$ samples. The relative centrifugal force (RCF) was set to 3000–9000 RCF and the rotation time was set to 60 s. The concentration factor was calculated as the number of bacteria observed in the bacterial trap/the number of loaded bacteria. The number of bacteria was counted after 30 min because it takes time for the bacteria to sink to the floor after rotation. The concentration factor was calculated by dividing the number of bacteria concentrated at the end of the channel by the total number of injected bacteria.

Bacterial capture and single cell tracking

A structure that can effectively trap floating bacteria in the culture medium was required. We attempted to solve this problem by introducing a special structure called the bacterial trap (Fig. 2c and d). The bacterial trap is a structure with a step that is dug deeper by approximately $50\text{ }\mu\text{m}$ from the bottom of the channel. Bacteria were concentrated at the end of the channel by centrifugal force spread over time, and the bacterial traps prevented the bacteria from spreading further away. In addition, the bacterial trap had a rectangular structure of $150\text{ }\mu\text{m} \times 250\text{ }\mu\text{m}$, which is similar to the field of

view of a 40× lens. Therefore, by focusing the microscope on the bottom part of the bacterial trap, bacterial division could be observed through time-lapse imaging (Fig. 1).

Image processing

To determine the resistance of bacteria to antibiotics, it is necessary to quantitatively count the number of bacteria by analyzing the microscopy images. However, it takes a significant time for the experimenter to count the bacteria. Moreover, in this process, errors may occur depending on the judgment criteria of the experimenter performing the AST. To overcome this limitation, we introduced automated image processing using an image processing program (ImageJ, NIH) to count bacterial cells.

Raw images were converted into gray-format images using a microscope (Fig. 4a). Images were cropped, and the brightness and contrast of the images were adjusted to make it easier to distinguish the bacteria (Fig. 4b and S5a†). The images were subsequently converted into binary images using the thresholding techniques of the image processing program (Fig. 4c and S5b–d†). Image thresholding was used to eliminate background noise. Areas where bacteria were present in the image were automatically measured using the program, and the number of bacteria was counted. The raw image data were converted into digital data and saved in an Excel file format (Fig. 4d and S5e–g†).

3. Results and discussion

Outlet-free-loading of the bacterial sample in the channel

Generally, an outlet is required to load the fluid into the microfluidic channel which vents air in the channel. However, when concentrating bacterial samples using a high centrifugal force, the samples are prone to leaking through the outlet. To solve this problem, we introduced a new technique called the outlet-free-loading technique (Fig. 5).

This method includes a bi-functional single-channel structure with inlet and outlet functions and sample-loading techniques using surface treatment for effective sample loading and pressure control inside the microfluidic channel.

The final microfluidic channel consisted of an exposed channel that served as an open-type reservoir and a sealed internal channel with a film to concentrate bacterial samples. To facilitate sample injection, the external channel must be hydrophobic, and the internal channel must be hydrophilic, and to this end, the surface of the external channel must be masked and the internal channel must be treated with oxygen plasma. Subsequently, only the plasma-treated part was sealed with the film to form a channel. Bacterial samples were loaded through an open channel. A small amount of the sample flowed into the hydrophilic inner channel and was no longer allowed to flow because of the air inside the sealed channel. To remove the air inside the channel, the chip was placed in a vacuum chamber and vacuum was applied. The air in the channel was discharged along with the sample toward the channel inlet. When the vacuum in the chamber was removed after sufficient air had been exhausted, all the bacterial samples entered the channel covered with the film. Subsequently, centrifugal force was applied to send the sample to the end of the channel and at the same time to concentrate it in the area where the bacteria were imaged.

Investigating the rehydration performance of the chip

Several tests were conducted to validate the rehydration performance of the dried antibiotics on the chip and the minimum RCF for moving the sample to the end of the channel. The bacterial samples were injected into the channel of a chip that was preloaded with dried antibiotics in the reservoir. Then, as the sample moved into the channel, it moved through the dehydrated antibiotic, dissolved the antibiotic, and reached the end of the channel. It could be

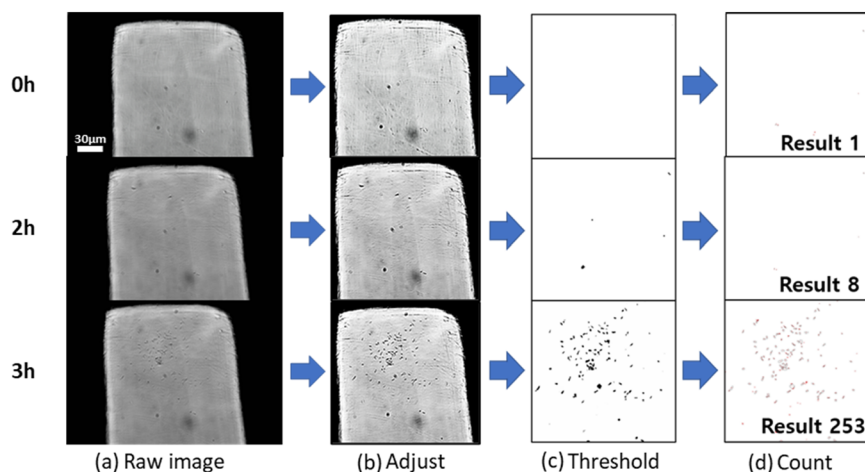


Fig. 4 Tracking the growth of *Escherichia coli* using time-lapse images and image processing. The bacteria were trapped and grew well in the bacterial trap. (a) Raw images were converted into grey format images. (b) Before the image processing, the brightness and contrast of the images were adjusted by the program to facilitate the identification of the bacteria. (c) Image thresholding was used to eliminate the background noise. (d) The number of bacteria was counted using ImageJ.

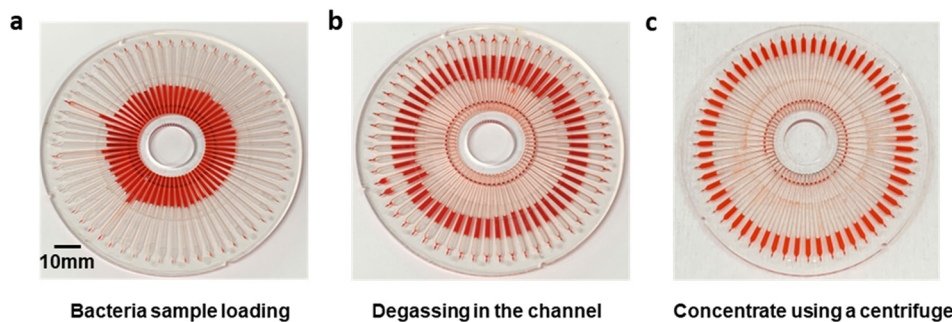


Fig. 5 Outlet-free-loading of the bacterial sample in the channel: (a) loading of bacterial sample; (b) removing air in the microfluidic channel; (c) concentration through a centrifuge. Scale bar represents 10 mm.

seen that the color of the injected bacterial sample gradually changed from orange to blue, which is the color of the dried dye on the channel. Thus, it was confirmed that the bacterial sample and dried antibiotic samples were properly mixed without other processes necessary (Fig. S6a†). In addition, to investigate the force required for the sample to reach the end of the channel, another experiment was conducted in various RCF ranges. Below 450 RCF, the sample did not move to the end of the channel. The minimum RCF at which the sample moved to the end was 450 RCF (Fig. S6b†).

Concentration performance according to the rotation speed

In this study, the bacteria were concentrated using centrifugal force. After the design optimization process by changing the length, depth, and width of the channel, we finalized the current design which is appropriate for the concentration of the bacterial sample and microscopic tracking. When the bacteria were concentrated, they were first collected from the end wall of the channel, sank by gravity and descended to the bottom of the well. The densities of the bacteria, $1.03\text{--}1.1\text{ g cm}^{-3}$,^{33,34} are higher than that of the MHB culture medium, 1.01 g cm^{-3} , but the difference in density was not large; therefore, the bacteria could be effectively separated only by applying a large centrifugal force. We verified the bacterial separation efficiency of the three strains. In the case of *E. coli*, the efficiency was approximately 13% at 3000 RCF and 62% at 7000 RCF. It did not increase significantly, even at 9000 RCF, and remained

approximately at 60%. The upper limit of RCF was set at 9000 because increasing the centrifugal force more than that could affect the viability of the bacteria.³⁵ In the case of *E. faecalis*, the efficiency was approximately 40% at 3000 RCF and was close to 80% at 7000 RCF. In the case of *S. aureus*, the efficiency was 35% at 3000 RCF, and nearly 90% at 7000 RCF (Fig. 6).

The concentration efficiencies of all three bacterial strains were lower at 9000 RCF than at 7000 RCF. In the case of 9000 RCF, the bond between the PET film and microfluidic chip could not withstand the centrifugal force and opened, and the bacteria leaked into the gap. Therefore, it was decided to use 6000 RCF when concentrating the bacteria because that force is sufficient to concentrate more than 60% of bacteria and has a negligible effect on the viability of the bacteria. The reasons for the loss of bacteria could be that 1) they are captured in between the film and chip and 2) adhered to the vertical wall. To increase the concentration factor, tighter bonding between the film and chip or changing the material of the chip to prevent adhesion could be applied. Bacteria with low motility settled to the bottom over time and could be observed, but it was difficult to track bacteria with good mobility, such as *P. aeruginosa* (Fig. S7†).

Rapid antibiotic susceptibility testing using microscopy imaging analysis

To validate the reliability of the system, we performed AST using our microfluidic AST chip from low

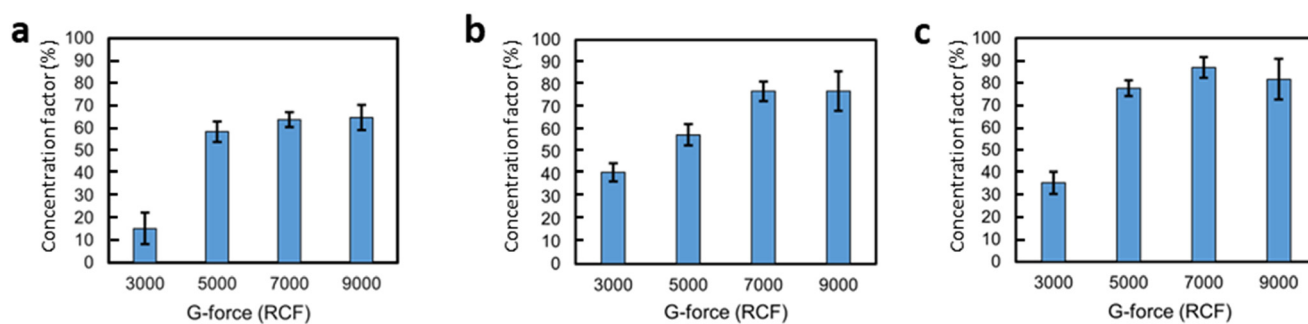


Fig. 6 Concentration factor of the centrifugal-based microfluidic chip with different bacteria and G-forces; (a) *Escherichia coli*, (b) *Enterococcus faecalis*, and (c) *Staphylococcus aureus*.

concentration bacterial samples of 10^3 and 10^4 CFU ml^{-1} . *E. coli* ATCC 25922 was tested against ampicillin, cefotaxime, and piperacillin as beta-lactam antibiotics and levofloxacin and amikacin as non-beta-lactam antibiotics. In addition, in all tests, a control case without antibiotics was added and used as a reference point to distinguish bacterial growth from non-growth. For *E. faecalis* ATCC 29212, ampicillin, levofloxacin, and piperacillin were selected, and for *S. aureus* ATCC 29213, amikacin, levofloxacin, cefotaxime, and piperacillin were selected as experimental antibiotics.

Fig. 7a shows the AST results for *E. coli* treated with ampicillin. Theoretically, when 10 μl of a sample with a concentration of 10^3 CFU ml^{-1} was concentrated and AST was performed, the number of bacteria present in the sample was approximately 10. Therefore, it was difficult to visualize the bacteria right after the concentration process. The bacteria were incubated (3–5 h) until they could be imaged, and then the number of bacteria was confirmed by analyzing the microscopy image. Due to the structure with a narrow channel and trap at the end of the channel, bacteria cells remained at the field of view for the incubation time (Fig. S8[†]).

In the case of *E. coli* with a concentration of 10^3 CFU ml^{-1} inoculated with ampicillin at 1 and 2 $\mu\text{g ml}^{-1}$, it was observed that the bacteria grew more than 20% compared to the control case. The basic test conditions of AST in our system are quite similar to those of the conventional broth microdilution test including the culture media and culture environment. Therefore, we followed the criteria from the CLSI for determination of growth of bacteria in the channel.⁶

However, when inoculated with antibiotics at a concentration of 4 $\mu\text{g ml}^{-1}$ or higher, a morphological change called filament formation occurred, which was determined to inhibit bacterial growth owing to the effect of antibiotics.³⁶ Based on these results, 4 $\mu\text{g ml}^{-1}$ was determined to be the MIC. In the case of levofloxacin, *E. coli* divided in the sample inoculated with 0.008 $\mu\text{g ml}^{-1}$ but not in the sample inoculated with 0.016 $\mu\text{g ml}^{-1}$ or more; therefore, the MIC value was determined to be 0.016 $\mu\text{g ml}^{-1}$ (Fig. 7b). When amikacin was inoculated with *S. aureus* at 10^3 CFU ml^{-1} , it was confirmed that the bacteria grew more than 20% at 0.5 $\mu\text{g ml}^{-1}$ compared to the control case. At a concentration of 1 $\mu\text{g ml}^{-1}$ or more, bacteria grew to less than 20% of the control case. Therefore, the MIC was determined to be 1 $\mu\text{g ml}^{-1}$

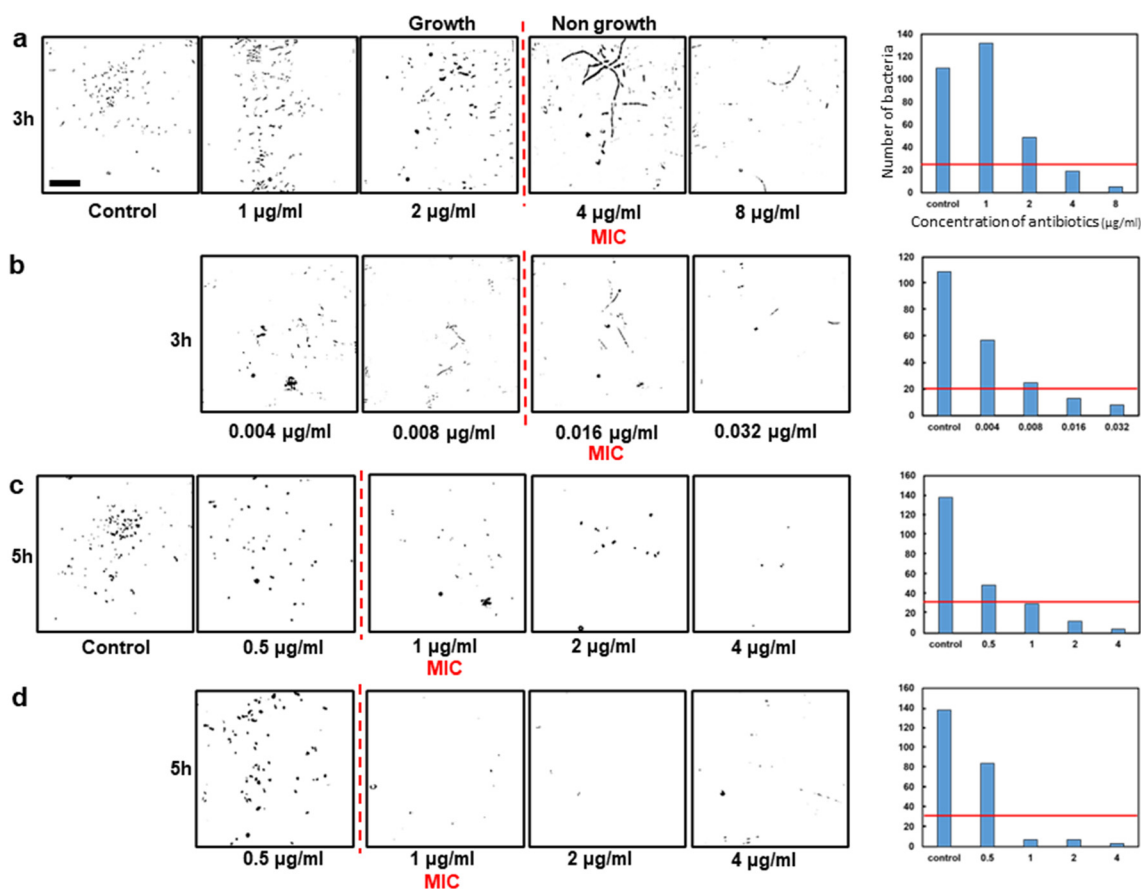


Fig. 7 Processed images and antimicrobial susceptibility testing (AST) data of *Escherichia coli* (10^3 CFU ml^{-1}) subjected to antibiotics at various concentrations; (a) ampicillin (b) and levofloxacin. (c) *Staphylococcus aureus* (10^3 CFU ml^{-1}) subjected to amikacin and (d) piperacillin. Scale bar represents 10 μm . Red lines in the graph represent the growth determination value which means 20% of the control case.

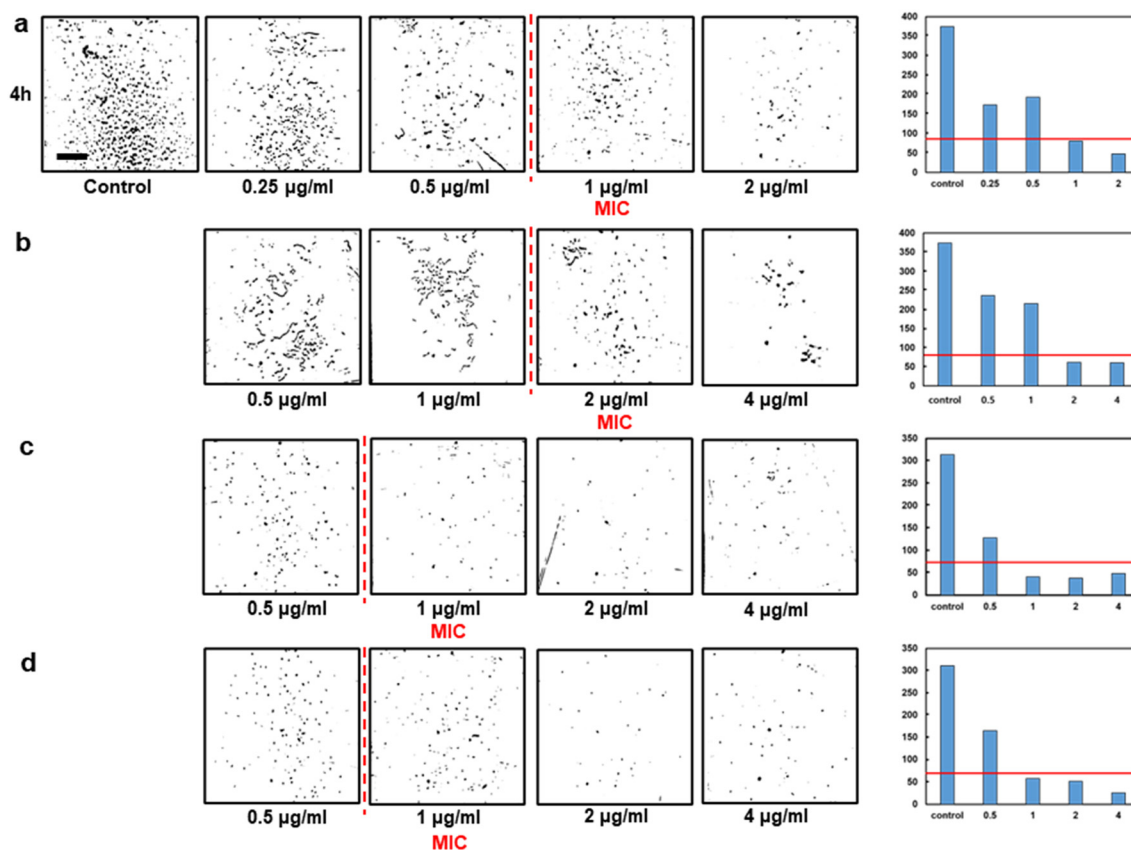


Fig. 8 Processed images and antimicrobial susceptibility testing (AST) data of *Enterococcus faecalis* (10^4 CFU ml^{-1}) subjected to antibiotics at various concentrations: (a) ampicillin and (b) piperacillin. *Staphylococcus aureus* (10^4 CFU ml^{-1}) subjected to (c) cefotaxime and (d) piperacillin. Scale bar represents 10 μm . Red lines in the graph represent the growth determination value which means 20% of the control case.

Table 1 MIC results of antibiotic susceptibility test (AST): (a) 10^4 CFU ml^{-1} concentration of the bacterial sample and (b) 10^3 CFU ml^{-1} concentration of the bacterial sample (unit: $\mu\text{g ml}^{-1}$)

	Bacteria (10^4 CFU ml^{-1})	Antibiotic	QC range	Chip	BMD test
a	<i>E. coli</i> (ATCC 25922)	Ampicillin	2–8	4	4
		Amikacin	0.5–4	4	0.5
		Cefotaxime	0.03–0.12	0.12	0.06
		Piperacillin	1–4	2	2
	<i>E. faecalis</i> (ATCC 29212)	Ampicillin	0.5–2	0.5	0.5
		Levofloxacin	0.25–2	1	0.25
		Piperacillin	1–4	2	1
	<i>S. aureus</i> (ATCC 29213)	Levofloxacin	0.06–0.5	0.25	0.25
		Cefotaxime	1–4	1	1
Piperacillin		1–4	1	1	
	Bacteria (10^3 CFU ml^{-1})	Antibiotic	QC range	Chip	BMD test
b	<i>E. coli</i> (ATCC 25922)	Ampicillin	2–8	4	2
		Levofloxacin	0.008–0.06	0.032	0.008
	<i>S. aureus</i> (ATCC 29213)	Amikacin	1–4	4	2
		Piperacillin	1–4	1	1

(Fig. 7c). Even when inoculated with piperacillin, bacterial growth was observed only at $0.5 \mu\text{g ml}^{-1}$; the MIC was determined to be $1 \mu\text{g ml}^{-1}$ (Fig. 7d). AST was performed using the above method, and the MIC was confirmed in a bacterial sample of 10^4 CFU ml^{-1} . The CLSI presents the BMD test as the gold standard for AST. Therefore, the

reliability of the AST results was determined by comparison with the BMD test. The MIC results of AST with the microfluidic AST chip and BMD test are shown in Fig. 8 and Table 1. In all cases, the AST results from the microfluidic AST chip is within the quality control (QC) ranges from CLSI as same as BMD tests.

Conclusion

In this study, low-concentration bacterial samples were concentrated on a microfluidic chip using centrifugal force, and the bacteria concentrated in a small area were observed under a microscope to derive AST results within a few hours. To perform sample loading, bacterial concentration, and microscopy imaging on one chip, outlet-free loading technology was introduced, enabling accurate AST with low-concentration samples and without the loss of bacteria. In addition, the AST results were automatically confirmed by extracting bacteria from the images of the bacteria through image processing. These technologies have suggested a method for performing drug testing in one step using clinical and environmental samples with various cell concentrations. In the case of bacteremia with very low concentrations of bacteria (~ 10 CFU mL⁻¹) in blood, an additional filtering process or separation process is needed to obtain a pure bacteria sample to perform AST in this platform. Since our device can be used even with a small concentration of bacterial samples compared to traditional methods, even if it undergoes additional culture, it can shorten the time required for testing compared to conventional methods. The current device is designed for multiplexed drug testing on a single chip. By changing the number of the chambers and size of the channel, this platform can be used in the case of a large sample volume. In the future, drug tests using mammalian cells may be another application method.

Conflicts of interest

The authors declare that they have no known competing financial interests or personal relationships that could have influenced the work reported in this study.

Acknowledgements

The authors gratefully acknowledge the support of the National Research Foundation of Korea (NRF) grant funded by the Korean Government (Grant No. 2022R1C1C1010059) and the support from the new faculty research fund of Ajou University.

References

- 1 T. U. Berendonk, C. M. Manaia, C. Merlin, D. Fatta-Kassinos, E. Cytryn, F. Walsh, H. Burgmann, H. Sorum, M. Norstrom, M. N. Pons, N. Kreuzinger, P. Huovinen, S. Stefani, T. Schwartz, V. Kisand, F. Baquero and J. L. Martinez, *Nat. Rev. Microbiol.*, 2015, **13**, 310–317.
- 2 E. Afshinnekoo, C. Bhattacharya, A. Burguete-Garcia, E. Castro-Nallar, Y. Deng, C. Desnues, E. Dias-Neto, E. Elhaik, G. Iraola, S. Jang, P. P. Labaj, C. E. Mason, N. Nagarajan, M. Poulsen, B. Prithiviraj, R. Siam, T. Shi, H. Suzuki, J. Werner, M. M. Zambrano, M. Bhattacharyya and S. U. B. C. Meta, *Lancet Microbe*, 2021, **2**, e135–e136.
- 3 J. H. Jorgensen and M. J. Ferraro, *Clin. Infect. Dis.*, 2009, **49**, 1749–1755.
- 4 K. Kocer, S. Klein, D. Hildebrand, J. Krall, K. Heeg, S. Boutin and D. Nurjadi, *J. Antimicrob. Chemother.*, 2021, **76**, 2795–2801.
- 5 M. R. Pulido, M. Garcia-Quintanilla, R. Martin-Pena, J. M. Cisneros and M. J. McConnell, *J. Antimicrob. Chemother.*, 2013, **68**, 2710–2717.
- 6 M. A. Wikler, F. R. Cockerill, K. Bush, M. N. Dudley, G. M. Elipoulos, D. J. Hardy, D. W. Hecht, J. F. Hindler, J. B. Patel, M. Powell, J. D. Turnidge, M. P. Weinstein, B. L. Zimmer, M. J. Ferraro and J. M. Swenson, *Clinical and Laboratory Standards Institute*, 2012, **26**, M07–A8.
- 7 R. M. Humphries, M. J. Ferraro and J. A. Hindler, *J. Clin. Microbiol.*, 2018, **56**, e00139-18.
- 8 T. J. J. Inglis and O. Ekelund, *J. Med. Microbiol.*, 2019, **68**, 973–977.
- 9 A. van Belkum, C. D. Burnham, J. W. A. Rossen, F. Mallard, O. Rochas and W. M. Dunne, Jr., *Nat. Rev. Microbiol.*, 2020, **18**, 299–311.
- 10 R. Datar, S. Orenga, R. Pogorelcnik, O. Rochas, P. J. Simmer and A. van Belkum, *Clin. Chem.*, 2021, **68**, 91–98.
- 11 J. Choi, H. Y. Jeong, G. Y. Lee, S. Han, S. Han, B. Jin, T. Lim, S. Kim, D. Y. Kim, H. C. Kim, E. C. Kim, S. H. Song, T. S. Kim and S. Kwon, *Sci. Rep.*, 2017, **7**, 1148.
- 12 Ö. Baltekin, A. Boucharin, E. Tano, D. I. Andersson and J. Elf, *Proc. Natl. Acad. Sci. U. S. A.*, 2017, **114**, 9170–9175.
- 13 J. Choi, J. Yoo, M. Lee, E. G. Kim, J. S. Lee, S. Lee, S. Joo, S. H. Song, E. C. Kim, J. C. Lee, H. C. Kim, Y. G. Jung and S. Kwon, *Sci. Transl. Med.*, 2014, **6**, 267ra174.
- 14 K. P. Smith, D. L. Richmond, T. Brennan-Krohn, H. L. Elliott and J. E. Kirby, *SLAS Technol.*, 2017, **22**, 662–674.
- 15 W. Kang, S. Sarkar, Z. S. Lin, S. McKenney and T. Konry, *Anal. Chem.*, 2019, **91**, 6242–6249.
- 16 J. Choi, Y. G. Jung, J. Kim, S. Kim, Y. Jung, H. Na and S. Kwon, *Lab Chip*, 2013, **13**, 280–287.
- 17 J. Q. Boedicker, L. Li, T. R. Kline and R. F. Ismagilov, *Lab Chip*, 2008, **8**, 1265–1272.
- 18 A. Tannert, R. Grohs, J. Popp and U. Neugebauer, *Appl. Microbiol. Biotechnol.*, 2019, **103**, 549–566.
- 19 Y. Yang, K. Gupta and K. L. Ekinci, *Proc. Natl. Acad. Sci. U. S. A.*, 2020, **117**, 10639–10644.
- 20 M. Mo, Y. Yang, F. Zhang, W. Jing, R. Iriya, J. Popovich, S. Wang, T. Gryns, S. E. Haydel and N. Tao, *Anal. Chem.*, 2019, **91**, 10164–10171.
- 21 A. Novelli-Rousseau, I. Espagnon, D. Filiputti, O. Gal, A. Douet, F. Mallard and Q. Josso, *Sci. Rep.*, 2018, **8**, 1–12.
- 22 H. Etayash, M. Khan, K. Kaur and T. Thundat, *Nat. Commun.*, 2016, **7**, 1–9.
- 23 C. Halford, R. Gonzalez, S. Campuzano, B. Hu, J. T. Babbitt, J. Liu, J. Wang, B. M. Churchill and D. A. Haake, *Antimicrob. Agents Chemother.*, 2013, **57**, 936–943.
- 24 T. Liu, Y. Lu, V. Gau, J. C. Liao and P. K. Wong, *Ann. Biomed. Eng.*, 2014, **42**, 2314–2321.
- 25 P. Stupar, O. Opota, G. Longo, G. Prod'Hom, G. Dietler, G. Greub and S. Kasas, *Clin. Microbiol. Infect.*, 2017, **23**, 400–405.

- 26 D. F. e Silva, A. Silva-Dias, R. Gomes, I. Martins-Oliveira, M. Ramos, A. Rodrigues, R. Cantón and C. Pina-Vaz, *Int. J. Antimicrob. Agents*, 2019, **54**, 820–823.
- 27 K. A. Stevens and L.-A. Jaykus, *Crit. Rev. Microbiol.*, 2004, **30**, 7–24.
- 28 V. Sunkara, S. Kumar, J. Sabaté Del Río, I. Kim and Y.-K. Cho, *Acc. Chem. Res.*, 2021, **54**, 3643–3655.
- 29 L. X. Kong, A. Perebikovsky, J. Moebius, L. Kulinsky and M. Madou, *J. Lab. Autom.*, 2016, **21**, 323–355.
- 30 J. Litvinov, S. T. Moen, C. Y. Koh and A. K. Singh, *Biomicrofluidics*, 2016, **10**, 014103.
- 31 C. J. Kim, D. Y. Ki, J. Park, V. Sunkara, T. H. Kim, Y. Min and Y. K. Cho, *Lab Chip*, 2020, **20**, 949–957.
- 32 I. Michael, D. Kim, O. Gulenko, S. Kumar, S. Kumar, J. Clara, D. Y. Ki, J. Park, H. Y. Jeong, T. S. Kim, S. Kwon and Y. K. Cho, *Nat. Biomed. Eng.*, 2020, **4**, 591–600.
- 33 M. Loferer-Krossbacher, J. Klima and R. Psenner, *Appl. Environ. Microbiol.*, 1998, **64**, 688–694.
- 34 L. R. Bakken and R. A. Olsen, *Appl. Environ. Microbiol.*, 1983, **45**, 1188–1195.
- 35 B. W. Peterson, P. K. Sharma, H. C. van der Mei and H. J. Busscher, *Appl. Environ. Microbiol.*, 2012, **78**, 120–125.
- 36 J. Choi, J. Yoo, M. Lee, E.-G. Kim, J. S. Lee, S. Lee, S. Joo, S. H. Song, E.-C. Kim and J. C. Lee, *Sci. Transl. Med.*, 2014, **6**, 267ra174.